132 *KSME International Journal, Vol. 12, No. 1, pp. 132~142, 1998*

Cooling Characteristics on the Forced Convection of an Array of Flat-form Electronic Components in Channel Flow

Kwang Soo Kim*, Won Tae Kim* and Ki Baik Lee**

(Received April 10, 1997)

Present study is concerned with forced convective heat transfer of the channel flow with line arrays of heated electronic components mounted on a printed circuit board. For the assessment of thermal performance in channel flows, three separate variables are used : channel spacing, row number of the component, and inlet air velocity. The thermal characteristics of a component due to own power and upstream air heated by components were studied. The experimental results were compared with those of numerical solution for various conditions : surface temperature of the components, adiabatic temperature rise, and heat transfer coefficient. The experimental results agree well with the numerical solutions. The study shows that the adiabatic heat transfer coefficient is significantly affected by the inlet velocity in channel flow and less dependent on the channel spacing and row number, except for the case of $H/B=3.3$. While reviewing the previous literatures, it is found that a little difference in the correlation between Nu and Re is due to the different geometric ratio of the packaged components.

Key Words: Adiabatic Heat Transfer Coefficient, Adiabatic Temperature, Electronic Cooling, Electronic Packaging

Nomenclature

A : Surface area of heated component (m^2)
B : Component height (m)
D_h : Hydraulic diameter (m)
H : Channel spacing (m)
h_{ad} : Adiabatic heat transfer coefficient (W/m^2°C)
i : Current across heated component (A)
k : Thermal conductivity (W/m°C)
L : Component length (m)
Nu : Nusselt number
Q_{cond} : Heat transfer rate by conduction (W)
Q_{conv} : Heat transfer rate by convection (W)
Q_{rad} : Heat transfer rate by radiation (W)
Re : Reynolds number
S : Component pitch (m)
T_{ad} : Adiabatic temperature of component (°C)
T_{in} : Inlet temperature of fluid (°C)
T_m : Mixed mean temperature of fluid (°C)
T_s : Surface temperature of heated component (°C)
T_∞ : Temperature far from heated component (°C)
ΔT_s : Surface temperature rise of the heated component (°C)
ΔT_{ad} : Adiabatic temperature rise of the heated component (°C)
V : Voltage drop across heated component (V)
V_{in} : Inlet velocity (m/s)
θ : Thermal wake function
ν : Kinetic viscosity (m^2/s)

* Electronic Packaging Technology Lab., ETRI (Electronics and Telecommunication Research Institute), P. O. Box 106, Yusong, Taejon 305-600
** Dept. of Mechanical Engineering, Pusan National Univ., Kumjong-Gu, Pusan 609-735

1. Introduction

The thermal management for electronics and electrical components has become an important and serious issue with the rapid increase of microchip power and power density. In the electronic packaging designs of power rated electronic components on printed circuit boards, specific consideration was given to the thermal analysis to achieve high heat dissipation rates. One of the typical component arrangements is mounting an array of components on printed circuit boards which are alternatively stacked. Since the mid of '80, there have been many researches for the forced convection on arrayed heated components (Sparrow et al., 1982; Ortega and Moffat, 1985).

Moffat and Anderson (1990) described the characteristics of the heat transfer coefficients based on temperature (T_∞) far from the heated surface, mixed mean temperature of the fluid (T_m) and the adiabatic temperature (T_{ad}) in line arrays. Anderson and Moffat (1990, 1992) obtained the adiabatic heat transfer coefficient (h_{ad}) using superposition kernel functions from the experiments and theoretical analysis, which proposed the applicable method in electronics cooling with non-uniform heat dissipation of components. Previous experimental work in electronics cooling has measured the heat transfer coefficients under the flow rate and channel spacing, which showed that heat transfer coefficients depends on Reynolds number based on the component length (Lehmann and Pembroke, 1991). From the extensive experiments conducted by Copeland (1992), the thermal wake functions were found to be strongly dependent on velocity and channel spacing. The reason why these results were not consistent seemed to be that in experiments different geometry in component height (B), component length (L), component pitch (S) and channel spacing (H) to compute heat transfer coefficients were applied. Even though there were reasonable amounts of data in the literature, each result showed a different correlation which seemed to be moderate to the geometry studied.

The main object of the present study is to investigate the adiabatic heat transfer coefficients and effects of thermal wake, both experimentally and numerically. Numerical works were carried out in coupling the adiabatic temperature rise with heating air coming from the upstream heated component in line arrays. These results can be used in thermal designs such as attaching the heat sink to the heated component or the rearrangement of the component location in the electronic packaging of the telecommunication system. The model in computational work can be extended to obtain a thermal wake function in a complex condition of heating and geometry.

In this study, heat transfer characteristics were obtained in the specified geometric array of 5×8 on printed circuit board (PCB) based on inlet velocity, channel spacing and row order. The following variables were used in the experiments : channel spacing ratio (H/B) ranging from 3.3 to 13.3 and Reynolds number based on component length from 3118 to 8314. In previous studies, most of the height of heated component relative to the component length were larger ($B\geq0.3L$), whereas configurations of the components considered on the PCB were square in flat-form with $B/L=0.09$ and $35(L)\times35(W)\times3(B)$ mm, modified actual memory or microprocessor with 3 mm thickness in a conventional way. In the view of the general telecommunication system, the channel spacing ranges from 10 to 40 mm and inlet velocity 1.5~4.0 m/s.

2. Experimental Apparatus and Procedure

2.1 Experimental apparatus

Figure 1 shows the experimental model of a coolant channel formed by PCB. The array of 5×8 were mounted on a rectangular PCB of epoxy glass with size of 415×295 mm, thickness of 1.6 mm and spacing of S=15 mm among components. After attaching each flat-form component to PCB, eight lead wires protruded from the component were inserted into the PCB and soldered. In PCB, electrical power was independently connected through the copper pattern for each row of the heated component. Each component was heated by a direct current passing through the thin layer of BeO. A sponge with 10 mm thickness filled a blank between PCB and an acrylic plate of 4 mm thickness located at the bottom. PCB

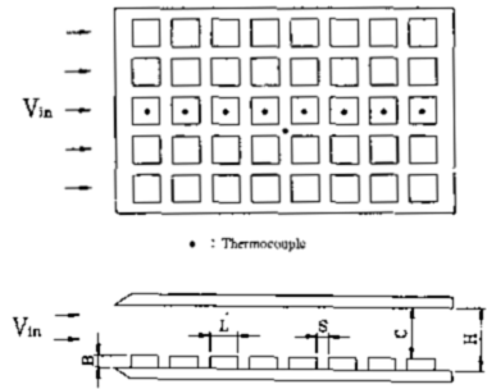

Fig. 1 Experimental model of coolant channel formed by printed cirduit board.

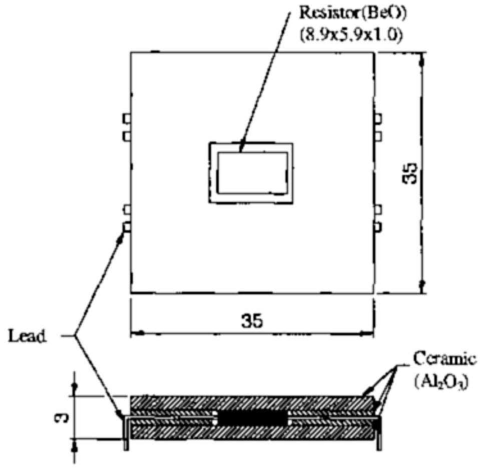

Fig. 2 Schematic of the heated component.

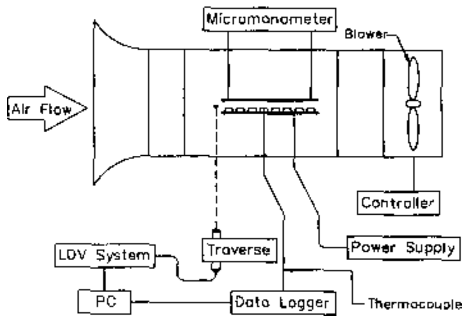

Fig. 3 Schematic of the experimental apparatus.

insulated with an acrylic plate was placed in a wind tunnel. The upper plate made by an acrylic plate of 4 mm thickness was varied at the distance of 10 mm from the desired channel spacing.

The special heater of a flat-form type applied to the heated component was manufactured as shown in Fig. 2. The heated component was consisted of a heating element made by BeO covered with alumina (Al_2O_3). The heating element of $8.9 \times 5.9 \times 1.0$ mm was inserted into a hole machined by laser cutting between alumina plates, and pasted by an epoxy bond.

The power to the heater was supplied by a variable auto-transformer (type HPS 60100, input 120V, output 0~60 V and up to 10 A). In the experiment, the electrical capacity of the heated component was achieved up to 100 W and 50Ω by controlling the variable auto-transformer. Even if the readings of the power have been recorded after the steady state was reached, a small fluctuation was observed ($\pm$0.05 V for voltage, $\pm$0.01 A for current).

The experimental set-up is schematically shown in Fig. 3. It is consisted of a wind tunnel, LDV (Laser Doppler Velocimeter, 2-D, fiber-optic type), power supply unit, and data acquisition system. From the wind tunnel, environmental air was flown into the channel. The size of the test section was 400×400 mm in cross section and 1,000 mm long. Inlet velocity entering the channel was measured by LDV system at the front side of the beginning of the channel. At the LDV with RSA-1000 processor, an ATS-600-3 traverse of 600 mm transfer distance was used in three-dimensional axes. After steady velocity and heating were obtained, the pressure drop across the test plate was measured with a micromanometer (FCO12, $\pm$0.05Pa), where two pressure taps were located at the first row close to the inlet from the ceiling of the upper channel and the eighth row close to the outlet. By controlling adjustable spacing, the channel distance between PCB and upper plate was varied.

To measure both surface temperature of the heated elements and air flows in the channel, the total 12 thermocouples (T-type, 40 AWG) were used. 8 thermocouples were embedded with the thermal bond (Thermalloy Inc., 4952) at the center of each top surface of 8 heated components arrayed in the middle column of PCB. For measuring the temperature of air entered through the wind tunnel, one thermocuple was placed at the inlet of the channel. The other two thermocouples were located for measuring the heat loss through PCB : one was attached to the top of the upper side of PCB and the other to the bottom of the lower side. To measure each temperature, a data logger of Campbell (CR-7) system was used with a PC for digitizing the results.

2.2 Experimental procedure

After setting the spacing between test channels to 10, 20, 30 and 40 mm at each experimental step, a series of tests for a given inlet air velocity were performed. The range of air velocity was from 1.5 to 4.0 m/s for each channel spacing. Once a flow rate in the wind tunnel was stablilized, various data were recorded. Inlet velocity of the test channel was finely measured from LDV system, which was traversed at several measuring points with the channel spacing at the inlet as shown in Fig. 3. The power to the heater was supplied in stages so that heated component maintained isothermal temperature rise. To monitor the temperature distributions of heated component and PCB, Thermo-Vision System (Agema, TVS-900) was specifically applied. Pressure drop between inlet and outlet was obtained for each test of the channel spacing and inlet velocity. After reaching a steady state under given experimental conditions, the surface temperature (T_s) of heated component at each row was measured. The adiabatic temperature (T_{ad}) as recommended from Moffat and Anderson (1990) was measured when its own power was off, but remainder of the components was "on." The term is not strictly accurate in a thermodynamics sense because there may be still heat transfer to or from the component by conduction, convection, or radiation with its surroundings; i. e., the component may not be truly adiabatic, but simply "unpowered." In spite of that defect in nomenclature, the term had will be used here.

The adiabatic heat transfer coefficient is defined as

$$h_{ad}=\frac{Q_{conv}}{A(\Delta T_s-\Delta T_{ad})} \tag{1}$$

where Q_{conv} is the heat transfer rate (W) by convection and is estimated using Eq'n. (2). A is the surface area of a heated component, ΔT_s is the surface temperature rise of the heated component, and ΔT_{ad} is the adiabatic temperature rise.

$$Q_{conv}=P-Q_{cond}-Q_{rad} \tag{2}$$

where P was calculated as $P=i$V, in which i is the current and V is the voltage drop across the heated component. The heat loss from the heated component through PCB, Q_{cond}, was estimated from the measurement of temperatures between the upper and lower plates of PCB, which were approximately 6.3 % of the input power. The radiation losses, Q_{rad}, were predicted to be within 1 % of the input power (Anderson and Moffat, 1990).

The heat transfer coefficient would mainly be a function of Reynolds number, a dimensionless channel spacing, and position in the array as follows :

$$Nu=f(Re,\ H/B,\ r) \tag{3}$$

In this equation, r is the row number and Nusselt number Nu is given as

$$Nu=\frac{h_{ad}L}{k} \tag{4}$$

where k is the thermal conductivity of air, and L is the component length. Furthermore, the Reynolds number Re is defined as

$$Re=\frac{V_{in}L}{\nu} \tag{5}$$

where ν is the kinetic viscosity of the air. All fluid properties were estimated at the inlet temperature.

There are several ways of choosing the characteristic length in this type of study. Anderson and Moffat (1990) chose the component height (B) as a characteristic length. On the other hand, Wirtz and Dykshoorn (1984) chose the component length (L), and Copeland (1992) chose the hydraulic diameter (D_h). In the present work similar to the geometry configuration adopted from Wirtz and Dykshoorn (1984) with a regular in-line array of flat packs (25.4×25.4×6.35 mm height), it was noted that the streamwise length of the heated component L was chosen as the characteristic length.

The uncertainty analysis was carried out for adiabatic heat transfer coefficient and Reynolds number. Also the preliminary experiments showed good repeatability during several runs under identical conditions. The errors involved in the calculation of heat transfer coefficient were generally due to the inaccuracy of the temperature and power measurements. Even if the readings of power and temperatures have been recorded after a steady state was reached, a little fluctuation was observed (± 0.05 V for voltage, ± 0.01 A for current, and $\pm 0.2\,^\circ$C for temperature). The analysis used is the standard single sample uncertainty analysis recommended by Kline and McClintock (1953). The uncertainty in the adiabatic heat transfer coefficient ranged from 9.1% at the smallest value of h to 4.4% at the largest. Also Reynolds number measured by LDV was estimated to be less than 3%.

3. Numerical Analysis

3.1 Mathematical modeling

The numerical model presented here was set in two-dimensions, but actual dimension was three-dimensional as shown in Fig. 1. Since the components were densely arranged in rows and columns, and component height was low, which affected the heat transfer of the side walls, it was assumed that the numerical model was two-dimensional. Also previous works (Dalvath and Bayazitoglu, 1987 ; Choi et al, 1994) had good results by two-dimensional analysis with this model. From the experimental Re_L ranging 3118 ~ 8314, standard k-ε turbulent model was taken. A conjugate analysis coupling the coolant flow with heat conduction in heated component and PCB was simulated.

The governing equations are described below. The mass conservation equation :

$$\frac{\partial}{\partial x_i}(\rho u_i)=0 \tag{6}$$

The momentum conservation equation :

$$\frac{\partial}{\partial x_j}(\rho u_i u_j)=-\frac{\partial p}{\partial x_i}+\frac{\partial \tau_{ij}}{\partial x_j} \tag{7}$$

$$\tau_{ij}=\mu_{eff}\left(\frac{\partial u_i}{\partial x_j}+\frac{\partial u_j}{\partial x_i}\right)-\frac{2}{3}\rho\chi\delta_{ij} \tag{7a}$$

$$\mu_{eff}=\mu+\mu_t \tag{7b}$$

The energy conservation equation :

In fluid

$$\frac{\partial(\rho c_p u_j T)}{\partial x_j}=\frac{\partial}{\partial x_j}\left(k_{eff}\frac{\partial T}{\partial x_j}\right) \tag{8}$$

$$k_{eff}=k+k_t \tag{8a}$$

$$k_t=\frac{\mu_t c_p}{Pr_t} \tag{8b}$$

In solid

$$\alpha_s\left(\frac{\partial^2 T}{\partial x_j \partial x_j}\right)_s+\left(\frac{\dot{q}}{\rho c_p}\right)_s=0 \tag{9}$$

The transport equation for k and ε :

$$\frac{\partial}{\partial x_i}(\rho u_i k)=\frac{\partial}{\partial x_i}\left(\Gamma_k\frac{\partial k}{\partial x_i}\right)+G-\rho\varepsilon \tag{10}$$

$$G=\mu_t\left(\frac{\partial u_i}{\partial x_j}+\frac{\partial u_j}{\partial x_i}\right)\frac{\partial u_i}{\partial x_j} \tag{10a}$$

$$\Gamma_k=\mu+\frac{\mu_t}{\sigma_k} \tag{10b}$$

$$\frac{\partial}{\partial x_i}(\rho u_i\varepsilon)=\frac{\partial}{\partial x_i}\left(\Gamma_\varepsilon\frac{\partial\varepsilon}{\partial x_i}\right)+C_1\frac{\varepsilon}{k}G-C_2\rho\frac{\varepsilon^2}{k} \tag{11}$$

$$\Gamma_\varepsilon=\mu+\frac{\mu_t}{\sigma_\varepsilon} \tag{11a}$$

The evaluation of turbulent eddy viscosity :

$$\mu_t=\rho C_\mu\frac{k^2}{\varepsilon} \tag{11b}$$

The empirical constants were, $C_1=1.44$, $C_2=1.92$, $C_\mu=0.09$, $\sigma_k=1.0$, and $\sigma_\varepsilon=1.3$.

As boundary conditions, inlet velocity was set to be 6 kinds added gradually with 0.5 m/s interval in the range of 1.5~4.0 m/s. The inlet temperature was set to the ambient temperature of 25°C. Neumann condition was set for the outlet boundary condition. The upper and lower acrylic plates of the flow channel were set to an adiabatic boundary condition. The heat from the resister as a source term was dissipated in the amount of 8.57×10^6 W/m³.

3.2 Numerical procedure

The numerical analysis using a generalized FLUENT computational code (Ver. 4.4.2, 1996) was performed. The numerical calculations were made with a grid size of 417 in x-direction, 26 ~47 for the channel space of 10~40 mm in y

-direction, of which maximum grids were totally given to 15,449. The finer grids were densely meshed close to the heated component. For fast motivation in the pressure term and energy equation, multi-grid correction was employed and under-relaxation coefficients were set to be 0.5 for velocity, 1.0 for pressure, and 0.8 for temperature.

It was assumed that the computation proceeded until the sum of the residuals for pressure, velocity, and turbulent variables from each iterative calculation was continuously reached less than 1.0×10^{-3}, and enthalpy residual was less than 1.0×10^{-6}. The computing iterations were taken about 8,500 more or less to run each case.

4. Results and Discussion

Figure 4 shows the numerical results for the isothermal lines based on Re with the geometric ratio H/B of 6.7 (meaning H=20 mm). In the figure, the temperature labeled at the bottom of each heated component ΔT_s means the increase in top surface temperature in the heated component with respect to inlet air temperature. The surface temperature near the entry evidently was decreased in all cases as the flow rate was increased and it was gradually increased as the flow goes downward near the exit. This is due to the effect of air heated from the upstream flow. Since the heat source for the heated component in the numerical solution is geometrically modeled as a power to the heater is supplied to only a resister located at the center of each component configured as shown in Fig. 2, the heat generated from the resister is dissipated to both component and PCB, in which the temperature difference in each component was found to be 2～3°C. These temperature distributions were coincident with those of the preliminary test conducted with Thermo-Vision System.

In Fig. 5, experimental results were compared with numerical solutions. This figure shows the surface temperature rise (ΔT_s) of the heated component to row number at H/B=10.0 for various Reynolds numbers. Both results obtained from the experiment and simulation matched well at high Reynolds number above about 6, 000. However, it was found that the computational results as Reynolds number decreases were higher by 2～4 ° C than those of experiment at downstream. It was predicted that the radiation heat loss in the experiment was larger for a high temperature component at a low velocity and in downstream regions than others. Also, since the

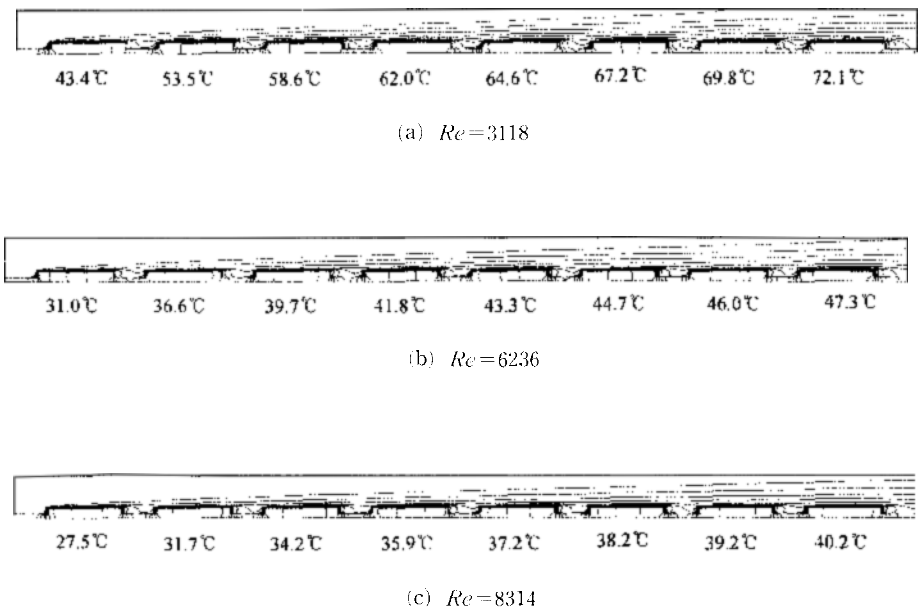

Fig. 4 Temperature field for H/B=6.7, paramenters in Reynolds number.

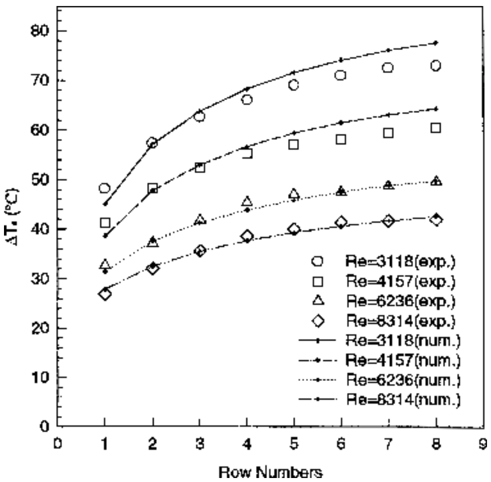

Fig. 5 Surface temperature rise vs. row number for $H/B=10.0$, parameters in Reynolds number.

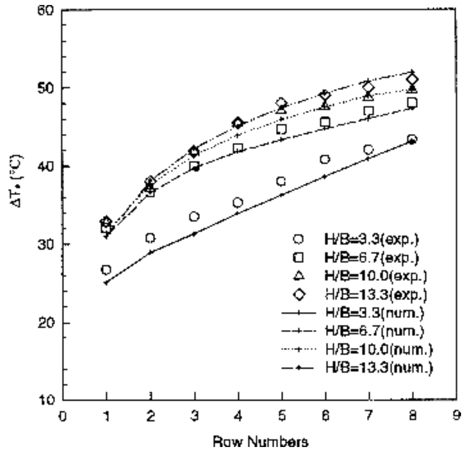

Fig. 6 Surface temperature rise vs. row number for $Re=6236$, paramenters in channel spacing ration (H/B).

lower bottom wall of a channel in computational modeling was under adiabatic condition, it was relatively more affected in low velocity regions.

The effect of geometric ratio of H/B from the experiments and computations is shown in Fig. 6. It shows the surface temperature rise at constant Reynolds number of 6,236 where inlet velocity is 3 m/s. It was clearly seen that the temperature rise did not have so much affect on changes of the channel spacing except the case of $H/B=3.3$. In general, a coolant entered over the component in the channel is divided into two regions : one of array region near the component and another of bypass region over the components. As the channel height increases for a fixed component height, the bypass height increases and the pressure drop decreases and more of the flow is diverted into the bypass region. As the channel height increases the velocity in the array decreases, thus decreasing heat transfer effectiveness. The amount of flow that passes through the array region is what determines the overall heat transfer from the components. Smaller channel results in more array region flow.

This result of Fig. 6 was a little different compared with the results reported from the previous literature (Wirtz and Dykshoorn, 1984; Anderson and Moffat, 1992). It could be explained that since channel spacing ratio (H/B) adopted in the present study is much larger compared to aforementioned literatures, the Reynolds number tends to have more effects than H/B on the surface temperature.

Figure 7 shows the adiabatic temperature rise (ΔT_{ad}) at $H/B=10.0$, in which ΔT_{ad} of component is created by convective heat transfer from the upstream warm air. From the results of this experiment, the temperature at the first row, although there was no heated component, was increased by 0.7~3.9°C due to pure conduction transfer through the surface of PCB. However, in the computational results for the first row, the adiabatic temperature rise was apparently not changed for any flow rate. It could be probably explained by that the convective heat transfer rate for the wall of PCB which was composed of copper cladding and glass filled with epoxy was arbitrarily set to a low value. For this reason, the computational result compared to the experimental result showed a comparatively lower value at the first row in the range of low Reynolds numbers in Fig. 5. With the heated component in the first row, adiabatic temperature rise of the downstream components was continuously stacked to be higher and decreased smoothly at the $7^{th}\sim 8^{th}$ row from the experimental results, while this phenomena did not appear in computations. From these results, it was predicted that at an exit

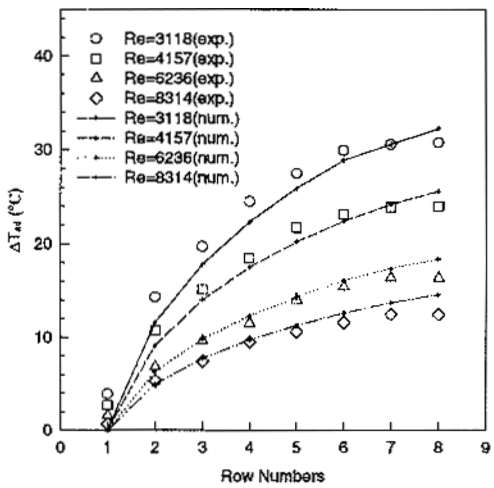

Fig. 7 Adiabatic temperature rise vs. row number for $H/B=10.0$, parameters in Reynolds number.

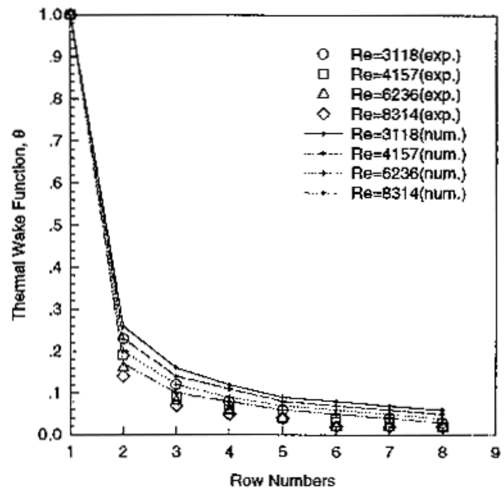

Fig. 8 Thermal wake function vs. row number for $H/B=10.0$, parameters in Reynolds number (only row 1 ; power on).

region there was no reverse conductive heat transfer, while convective heat transfer still existed actively.

The temperature rise downstream component depends upon its relative location, flow conditions, and heat dissipation rate of neighbors. The thermal wake function is defined in a non-dimensional form as follows :

$$\theta_i=\frac{T_i-T_{in}}{T_{rh}-T_{in}} \tag{12}$$

where $T_{rh}-T_{in}$ is the temperature rise of the heated component residing at row number $r=rh$, and T_i-T_{in} is the temperature rise of a downstream component with i which is the number of rows downstream from the heated component.

Influences of the thermal wake on other rows by one heated component on the first row were demonstrated in Fig. 8. The heat generated on the first row only and the heat was transferred to downstream components. The heat was considerably transferred through the conjugate phenomena by the heated first component in the adjacent $2^{nd}\sim4^{th}$ rows and in the far downstream evolution the temperature rise was uniform approaching 4～8%. This thermal wake function can be used in order to predict the surface temperature rise in the line arrays of heated component by superposition.

Figures 9 and 10 showed the data from each row of an array for $HB=10.0$ and $Re=6{,}236$. The adiabatic heat transfer coefficients were obtained from the deduction of the adiabatic temperature of Fig. 7, and also from the surface temperature rise of Fig. 5, in which the convection cooling performance on the heated component itself at each row, removing the upstream flow effect, was estimated.

From the experimental results shown in Fig. 9, the heat transfer coefficient at the first row was the peak at $Re=8{,}314$ and at $Re=3{,}118$ and 4, 157 under the same condition of the lowest level, which were consistent with previous works (Anderson and Moffat, 1990, 1992). In general, a coolant entered over the component in the channel is divided into two regions : one of array region near the component and another of bypass region over the component. As shown in Fig. 9, with a large channel spacing ratio of H/B and a relatively low inlet velocity, a coolant entered through the inlet did not fully pass to the array region and mostly passed the bypass region at the first row in line arrays. However, as the inlet velocity is increased, the flow went mostly through the array region, making thermal performance for the electronics cooling enhanced. The

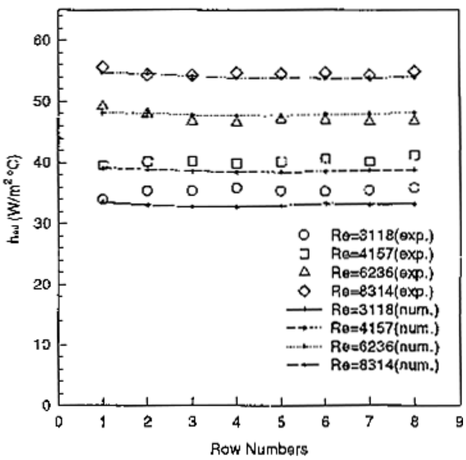

Fig. 9 Adiabatic heat transfer coefficient vs. row numbers for $H/B=10.0$, parameters in Reynolds number.

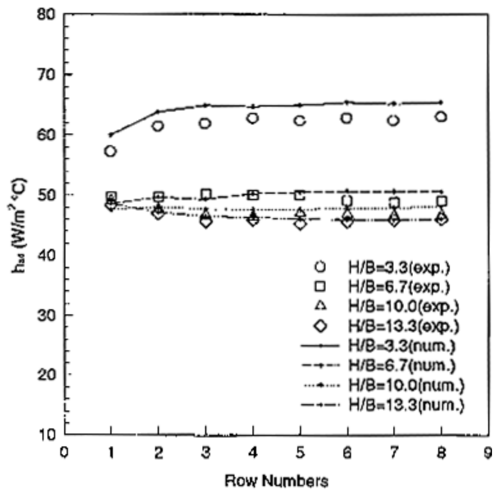

Fig. 10 Adiabatic heat transfer coefficient vs. row numbers for $Re=6236$, parameters in channel spacing ratio (H/B).

computational results showed that a for all heated components in line arrays, cooling was uniformly performed, and most of the results agreed well with those of experiment.

In Fig. 10, the adiabatic heat transfer coefficient is shown in line arrays for different channel spacing. As shown in the behavior described in the figure, the heat transfer coefficients were independent on the channel spacing except for $H/B=3.3$. This result was not consistent with that of previous works (Anderson and Moffat, 1990, 1992) reporting that the heat transfer coefficient was increased while decreasing the channel spacing. It would be predicted because as aforementioned in Fig. 6 most of the coolant at high H/B (6.7~13.3) passed through the bypass region not the array region. It also could be proved by the velocity profile at the boundary of the component. Although same velocity at the inlet for different H/B, the velocity profile inside the channel was different. When we analyzed the velocity profile from numerical results, the velocity of the boundary layer on the component at low H/B was higher than at high H/B.

Nusselt number (Nu) and Reynolds number (Re) were defined in terms of mean heat transfer coefficients and inlet velocity measured, respectively, and Nu-Re correlation of the parameters in the channel spacing ratio was depicted in Fig.

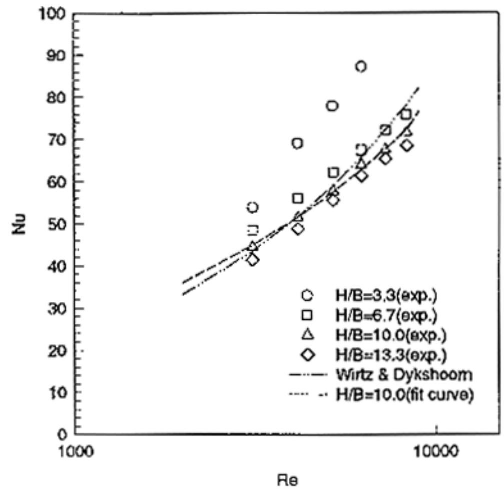

Fig. 11 Variarion in Nusselt number with respect to Reynolds number (this study & reference).

11. The correlation of Nu versus Re, $Nu=0.487\,Re^{0.59}$, at the channel spacing ratio (H/B) of 3.3 was well coincident with $Nu=0.346Re^{0.6}$ in inclination 0.59 and 0.6, which was reported by Wirtz and Dykshoorn (1984) who tested the inlet velocity concept on their data from "sparse flat-packs" of H/B of 1.25~4.5.

But the correlation from the different geometry of H/B of 6.7~13.3 was slightly different from that of Wirtz and Dykshoorn (1984). The inclinations were nearly same as 0.46, 0.49, and 0.51 at 6.7, 10.0, and 13.3 of H/B, respectively. This range of H/B was conventionally used in the telecommunication system, and the correlation at $H/B=10.0$, their intermediate channel spacing ratio, by curve fitting, was shown as follows :

$$Nu=0.890Re^{0.49} \tag{13}$$

5. Conclusions

From the experimental and numerical study, the surface temperature rise, adiabatic heat transfer coefficients, and the affects of thermal wake on line arrays of flat-form components have been considered, and following conclusions are made:

(1) For the surface temperature rise of the heated components, the adiabatic temperature rise, and the adiabatic heat transfer coefficient, all data obtained from experiment and computation agreed well. It could be established as a benchmark for two-dimensional computation for this electronic channel model.

(2) In case of higher H/B by 6.7, the adiabatic heat transfer coefficient (h_{ad}) was mostly independent of the channel spacing, but considerably affected the inlet velocity.

(3) At one heated component and another with the power off, the affects on thermal wake were considerable in both upstream flow and conductive heat transfer through PCB until the 3rd row in line arrays, and in the downstream evolution the temperature rise was kept consistently.

(4) The correlation between Nu and Re was presented to make possible the direct calculation of the adiabatic heat transfer coefficient on a non-uniform heated array.

Specially, the developed numerical method in the present study could be extended to more complex conditions of heating and geometry, such as attaching heat sink on the heated components.

Acknowlegement

This work was supported as a project of ATM system development, HAN/B-ISDN. The authors really appreciate the support.

References

Anderson, A. M. and Moffat, R. J., 1990, "Convective Heat Transfer from Arrays of Modules with Non-uniform Heating Experiments and Models," *Stanford Univ.*, Report No. HMT-43, pp. 126, 175.

Anderson, A. M. and Moffat, R. J., 1992, "The Adiabatic Heat Transfer and the Superposition Kernel Function," *ASME J. of Electronic Packaging*, Vol. 114, pp. 14~28.

Biber, C. R. and Sammakia, B. G., 1986, "Transport from Discrete Heated Components in Turbulent Channel Flow," *ASME Preprint 86-WA/HT-68*, pp. 1~9.

Choi, C. Y., Kim, S. J., and Ortega, A., 1994, "Effect of Substrate Conductivity on Convective Cooling of Electronic Components," *ASME J. of Electronic Packaging*, Vol. 116, pp. 198~205.

Davalath, J. and Bayazitoglu, Y., 1987, "Forced Convection Cooling Across Rectangular Blocks," *J. of Heat Transfer*, Vol. 109, pp. 321~328.

David Copeland, 1992, "Effects of Channel Height and Planar Spacing on Air Cooling of Electronic Components," *ASME J. of Electronic Packaging*, Vol. 114, pp. 420~424.

Fluent Inc., 1996, *Fluent User's Guide*(V. 4.4).

Garimella, S. V. and Eibech, P. A., 1990, "Heat Transfer Characteristics of of an Array of Protruding Components in Single Phase Forced Convection," *International J. of Heat and Mass Transfer*, Vol. 33, pp. 2659~2670.

Kline, S. J. and McClintock, 1953, "Estimating Uncertainty in Single-Sample Uncertainty Analysis," *Mechanical Engineering*, Jan., pp. 3~8.

Lehmann, G. L. and Pembroke, J., 1991, "Forced Convection Air Cooling of Simulated Low Profile Electronic Components," *ASME J. of Electronic Packaging*, Vol. 113, pp. 21~26.

Lehmann, G. L. and Wirtz, R. A., 1985, "The Effect of Variations in Streamwise Spacing and Length on Convection from Surface Mounted Rectangular Components," *Heat Transfer in*

Electronic Equipment, ASME HTD, Vol. 48, pp. 39～48.

Moffat, R. J. and Anderson, A. M., 1990, "Applying Heat Transfer Coefficient Data to Electronics Cooling," *J. of Heat Transfer,* Vol. 112, pp. 882～890.

Ortega, A. and Moffat, R. J., 1985, "Heat Transfer from Array of Simulated Electronic Component : Experimental Results for free Convection with and without Shrouding Wall," *Heat Transfer in Electronic Equipment, ASME HTD,* Vol. 48, pp. 5～16.

Sparrow, E. M., Niethhammer, J. E. and Chaboki, A, 1982, "Heat Transfer and Pressure Drop Characteristics of Arrays of Rectangular Modules Encountered in Electronic Equipment," *Int. J. of Heat and Mass Transfer,* Vol. 25, No. 7, pp. 961～973.

Wirtz, R. A. and Dykshoorn, P., 1984, "Heat Transfer from Arrays of Flat Packs in a Channel Flow," *Proceedings of the Fourth Annual International Electronics Packaging Society,* Baltimore, pp. 318～326.